

Indecomposable continua in dynamical systems with noise: Fluid flow past an array of cylinders

Miguel A. F. Sanjuan

Institute for Physical Science and Technology, University of Maryland at College Park, College Park, Maryland 20742, and Departamento de Física e Instalaciones Aplicadas, E.T.S. de Arquitectura, Universidad Politécnica de Madrid, 28040 Madrid, Spain

Judy Kennedy

Department of Mathematical Sciences, University of Delaware, Newark, Delaware 19716

Celso Grebogi and James A. Yorke

Institute for Physical Science and Technology, University of Maryland at College Park, College Park, Maryland 20742

(Received 6 June 1996; accepted for publication 19 September 1996)

Standard dynamical systems theory is based on the study of invariant sets. However, when noise is added, there are no bounded invariant sets. Our goal is then to study the fractal structure that exists even with noise. The problem we investigate is fluid flow past an array of cylinders. We study a parameter range for which there is a periodic oscillation of the fluid, represented by vortices being shed past each cylinder. Since the motion is periodic in time, we can study a time-1 Poincaré map. Then we add a small amount of noise, so that on each iteration the Poincaré map is perturbed smoothly, but differently for each time cycle. Fix an x coordinate x_0 and an initial time t_0 . We discuss when the set of initial points at a time t_0 whose trajectory $(x(t), y(t))$ is *semibounded* (i.e., $x(t) > x_0$ for all time) has a fractal structure called an *indecomposable continuum*. We believe that the *indecomposable continuum* will become a fundamental object in the study of dynamical systems with noise. © 1997 American Institute of Physics. [S1054-1500(97)01701-1]

Fractal structures appear naturally in nonlinear dynamical systems. These structures are typically invariant sets in the sense that they are unchanged under the time evolution of the dynamical system. It has been found¹ that many fractal sets in dynamics can be classified topologically as being indecomposable continua. In this paper, we bring fundamental properties from topology, properties that apply to indecomposable continua, to understand fractal invariant structures that arise in dynamics. We choose a specific physical situation, that of a fluid flow past an array of cylinders, to study the invariant fractal sets formed in the wake of the cylinders. In particular, we use topological properties of indecomposable continua to prove that these fractal structures persist under the influence of noise.

I. INTRODUCTION

The standard approach to studying dynamical systems is to study invariant sets, such as attractors, basin boundaries, stable and unstable manifolds, fixed points, periodic orbits, and chaotic saddles. When we add a small amount of random noise, these invariant sets are destroyed. We attempt to describe other sets which remain despite the noise. To illustrate the ideas we investigate a rich example: an incompressible flow past an infinite sequence of cylinders. We create a plausible stream function and study its Lagrangian dynamics. Using the Navier-Stokes equations would be preferable, but they are computationally too difficult to solve since we follow trajectories for long time periods and compute stable and

unstable manifolds. In our Lagrangian dynamics we model a fluid whose velocity field fluctuates periodically, perhaps with some random fluctuations added. We focus on the dynamics and topology inherent in this model.

The model itself is formulated with the help of a stream function in such a way that the velocity field equations of the fluid flow are formally identical to Hamilton's equations. In these equations, the stream function plays the role of a time-dependent Hamiltonian. They describe the motion of the trajectories of a fluid particle in an incompressible two-dimensional flow. A schematic diagram of the numerical experiment appears in Fig. 1, with extensive details provided in Sec. IV. Fluid flows downstream, from left to right in the figure, but points inside and on the boundaries of the cylinders are fixed, and the cylinder obstacles cause the complications in the flow. Far away from the cylinders, above and below, the flow is nearly laminar, but of course when the fluid encounters the cylinders, chaos arises (see Fig. 2).

Our goal is to study the sets $S^+(x_0)$ and $S^-(x_0)$. The set $S^+(x_0)$ is defined to be the set of points (x, y) at time $t_0 = 0$ with the property that the trajectory $(x(t), y(t))$ satisfies $x(t) \geq x_0$ for all time (positive and negative). The points in $S^-(x_0)$ have trajectories satisfying $x(t) \leq x_0$ for all time. Notice that $S^+(x_0)$ include all the cylinders to the right of x_0 . As we explain later we add the point at ∞ in the plane to the sets $S^+(x_0)$ and $S^-(x_0)$, so that they are compact sets. Most trajectories flow from $x = -\infty$ to $x = +\infty$. We carry this even further though, in that our primary aim is to describe the topology of the sets of semibounded trajectories in the presence of small random fluctuations in the flow.

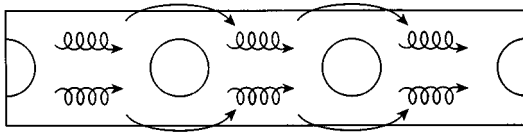


FIG. 1. The figure shows an array of cylinders, where the fluid flows downstream. Vortices are shed periodically behind each cylinder, they move along the channel and they die out. In most of our pictures the vertical scale is changed so the cylinders appear highly elliptical. The horizontal lines show the range of y used in all the figures.

We simplify the problem by using the periodicity and symmetry inherent in the example and then consider the time-1 Poincaré return map, since the period of the flow is $T=1$. Thus, the flow is converted into a discrete-time map of the plane to itself. When considering the discrete-time map induced by the flow, we study the invariant sets in the dynamics, and when we consider perturbations of that flow, we study the semibounded trajectories. Our investigation involves numerical studies of the model first, followed by a rigorous investigation of the sets suggested by the numerical studies. Of course none of our numerical observations are rigorous so we carefully specify axiomatically in Secs. II and III what observations would imply what conclusions.

A *continuum* is a compact, connected metric space. It is called *decomposable* if it is the union of two overlapping proper subcontinua; otherwise, it is called *indecomposable*. The first question that might arise is whether indecomposable continua do exist. The continua that automatically jump to mind, such as a line segment or a disk, are decomposable. A piece of chalk is a decomposable continuum; if you break it, you have two pieces from which it was composed. On the other hand, every indecomposable continuum has the property that if it were separated in half, it would shatter into an uncountable number of pieces, each nowhere as dense as in the original continuum. This property can be used to define

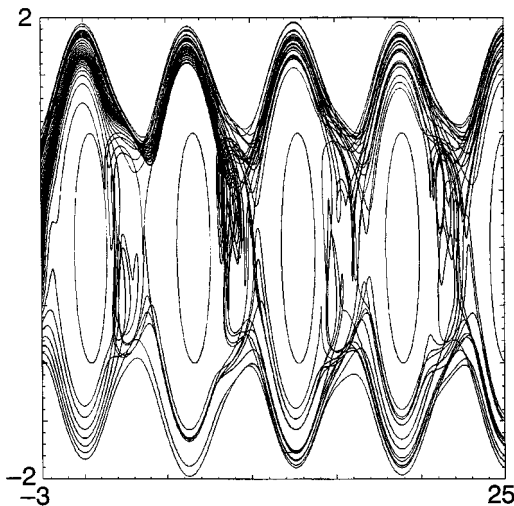


FIG. 2. Several continuous time trajectories are shown, illustrating the chaos between cylinders.

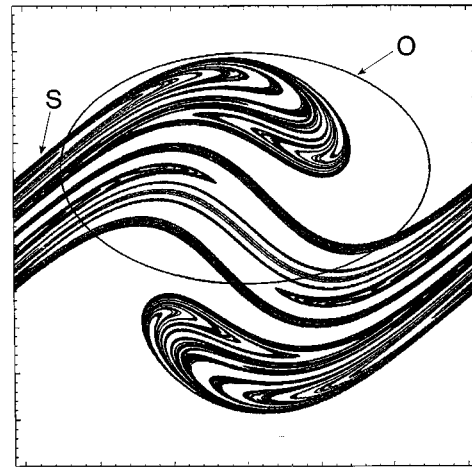


FIG. 3. A continuum S is indecomposable if for every open set O that intersect S (with some part of S lying outside the closure of O), the intersection $O \cap S$ has infinitely many pieces. This figure shows a typical strange attractor on a cylinder. (The right side of the pictures coincide with the left.) This picture was generated using equations of a parametric pendulum.

the term (see Fig. 3). Indecomposable continua often occur in dynamical systems. Examples include most connected strange attractors and many basin boundaries. Here we do not have attractors or basin boundaries, but we still have indecomposable continua. An introduction to such sets is provided in Appendix A at the end of the paper.

Much of the set $S^+(x_0)$ often can be approximated as follows. At time $t_0 \ll 0$, pour dye into the fluid along the vertical line through $x=x_0$. Most of it is rapidly swept downstream but trace amounts remain, and their remnants lie near $S^+(x_0)$. The more negative the time t_0 is for introducing the dye, the closer the remnants lie to $S^+(x_0)$, but also there is much less dye that has not yet been swept downstream.

We conjecture that in many circumstances, if the two-dimensional flow is sufficiently fast and irregular, the semi-bounded sets include indecomposable continua. The set $S^+(x_0)$ shown in Fig. 4 is an indecomposable continuum in our example.

Our efforts to analyze this fluid flow is greatly simplified when we can find some location, some vertical lines, at which the flow is strictly downstream. In our example, we could have chosen the vertical line through the cylinder, but a less trivial example of such a line is shown in Figs. 4 and 5. When we discuss $S^+(x_0)$, we prefer to think of x_0 as such an x -coordinate when the flow is uniformly downstream.

We observe that the time-1 Poincaré map has a horseshoe and therefore has an invariant set between each pair of consecutive cylinders (see Fig. 6). As is well known, such an invariant Cantor set possesses properties of topological self-similarity. The indecomposable continuum contains this invariant Cantor set and also has these properties of topological self-similarity. One of the results we establish is the following “nesting property.” Between a consecutive pair of cylinders the time-1 map is a horseshoe map on a quadrilateral Q_0 and Q_0 has an invariant Cantor set and an associated indecomposable continuum Λ_0 in $S^+(x_0)$. We claim (Propo-

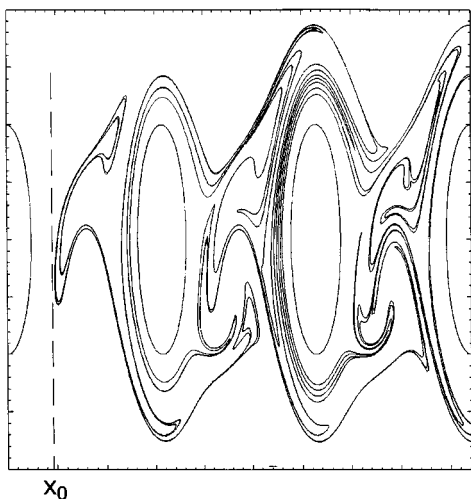


FIG. 4. The set shown $S^+(x_0)$ is the set of points whose trajectories remain for all time ($t=0, \pm 1, \pm 2, \dots$) to the right of the dashed line at $x=x_0$.

sition 2.4) that in any geometry like that of our example, the set Λ_0 includes the downstream, indecomposable continua Λ_n in $S^+(x_0 + 2n\pi)$ for $n=1, 2, \dots$. In our case Λ_n is a horizontal translate of Λ_0 translated by $x=2\pi n$. Moreover we claim (Theorem 3.4) that the addition of a small amount of random perturbation does not affect the relationship $S^+(x_0) \supset S^+(x_0 + 2\pi) \supset \dots$, and these sets must still contain indecomposable continua.

In general the essential features of $S^+(x_0)$ are not destroyed by small perturbations in the system. We refer to this as the *fish factor*, i.e., how a collection of small fish swimming randomly, nonperiodically, but close to the cylinders affects the flow and the sets of semibounded trajectories. In a

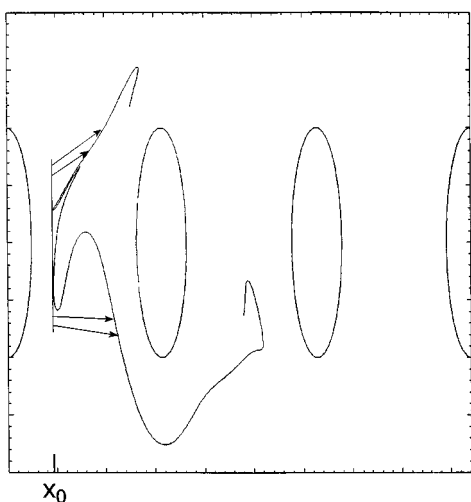


FIG. 5. The value x_0 was chosen carefully in Fig. 4 so that all points on it are mapped to the right by the time-1 map F . The curve shown is the image of this segment shown at $x=x_0$. While it is hard to see, there is a gap between this line segment and the image, so that the segment maps strictly to the right.

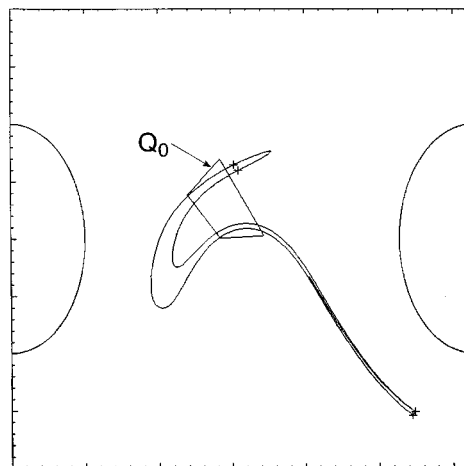


FIG. 6. This figure shows a horseshoe. The crosses are the images of the vertices of the quadrilateral Q_0 under the action of the map G . This map G is a special map that is the ‘‘square root’’ of F , that is, $G(G(x, y)) = F(x, y)$ for all $(x, y) \in Q_0$. See Appendix B for an explanation of why $F = G^2$.

real-life situation, no periodic process is likely to describe fluid flow. At the very least, small time-dependent perturbations from that model occur. Thus, we can think of applying, instead of one particular map F over and over again, a sequence of maps F_i . These maps F_i denote the maps applied at time i , and $F_i(u)$ are close to $F(u)$ for all i and all u , and each F_i fixes the points of the cylinder. In this case, it no longer makes sense to talk about periodic points and invariant sets, since no single map is involved. It still makes sense to talk about the sets $S^+(x_0)$ and $S^-(x_0)$. We also investigate the connection between $S^+(x_0)$ and $S^-(x_0)$. The intersection of these two indecomposable sets $S^+(x_0)$ and $S^-(x_0 + 2\pi)$ contains Cantor sets, a cylinder and some invariant bubbles of fluid (see Fig. 7).

We observe in our example, see Fig. 8, a feature that is very helpful when analyzing such flows with noise, namely there is a vertical line at $x=\bar{x}_0$ to the right of the quadrilateral Q_0 with properties described in the figure captions. These features imply that something very similar must be true for any process \tilde{F} , with a small amount of noise, namely if $q \in Q_0$ and $\tilde{F}(q) \notin Q_0$, then $\tilde{F}^n(q)$ is to the right of \bar{x}_0 for all $n=2, 3, 4, 5, \dots$.

While Fig. 6 shows $G(Q_0)$, Fig. 9 shows $F(Q_0)$. Figure 10 shows the invariant Cantor set in Q_0 . This Cantor set is the intersection of stable and unstable manifolds, see Fig. 11.

The dynamics of G inside the quadrilateral are exactly the same, from both a topological and dynamical perspective, as those of the standard Smale horseshoe map. However, the *geometry* of what goes on *outside* of that quadrilateral is quite different and more complicated than it is for the Smale horseshoe. While the geometry associated with the smallest Smale horseshoe yields the simplest type of indecomposable continuum, (see Appendix A), this geometry yields one with more interesting structure. As described in Fig. 8, any point q which leaves the quadrilateral Q_0 , must ‘‘flow’’ downstream under iteration by F . In particular, it

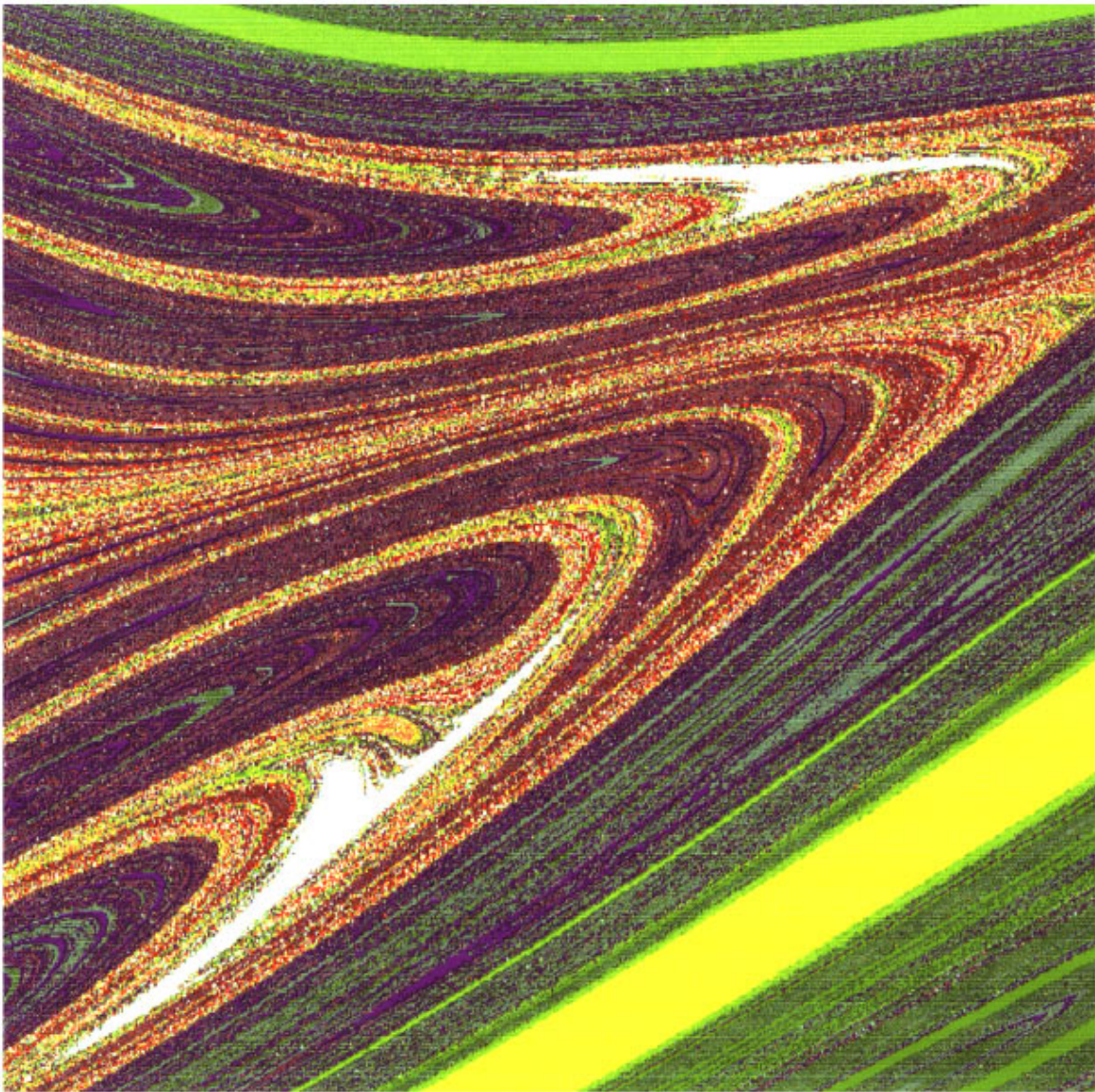


FIG. 7. This figure shows the exit times, the time required to pass to the next cylinder, in different colors in the region $1.25 < x < 1.7$ and $-0.6 < y < 0.5$. This region is to the immediate right of a cylinder, the two invariant bubbles (white) are clearly visible in this region. Solid colored regions have small exit times, while the brown speckled regions have long exit times.

cannot reenter Q_0 . It can then either get “stuck” in the stream around some downstream invariant set (Cantor set, cylinder, or bubble), or, more likely, flow towards ∞ . Points do not “flow” very far upstream. However, if one considers the time-reversal map F^{-1} , then another indecomposable continuum $S^-(x_0)$ results, an upstream continuum again containing the point ∞ . Of course $S^-(x_0 + 2\pi)$ is a translate of $S^-(x_0)$, because the process is periodic in x with period 2π .

The paper is organized as follows. In the next section we discuss our main results about how the indecomposable continua arise in the fluid flow. Section III discusses how these results change when we add a small amount of noise. We note that there is a large literature on perturbed dynamical systems of various kinds, but it does not address indecomposable continua of noisy systems. Section IV explains the

details of the stream function which models the velocity field of the flow past an array of cylinders. Section V provides our concluding remarks. Appendix A provides the basic topological ideas needed to understand indecomposable continua, and Appendix B describes why there is a map G with the property $G^2 = F$.

II. INTERMINGLING INDECOMPOSABLE CONTINUA IN THE CYLINDER FLOW

In this section we take an axiomatic approach to the fluid flow. We assume there is a time-1 diffeomorphism $F: R^2 \rightarrow R^2$. We employ the so-called one point compactification of R^2 . We add the point ∞ to R^2 and we write $\overline{R^2} = R^2 \cup \{\infty\}$. We say the sequence u_i in R^2 converges to ∞ if and only if $|u_i| \rightarrow \infty$ as $i \rightarrow \infty$. The space $\overline{R^2}$ is compact.

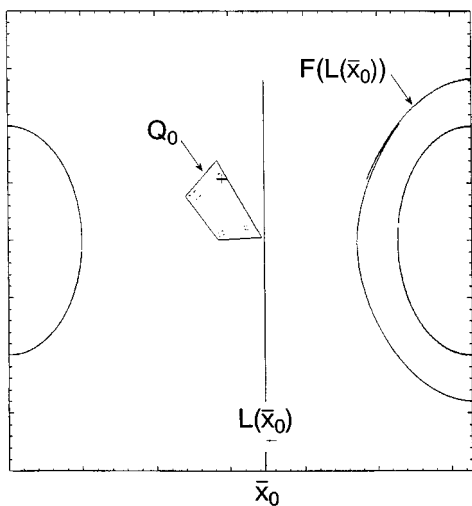


FIG. 8. In our example the vertical line $L(\bar{x}_0)$ (shown above with x -coordinate \bar{x}_0) has the property discussed in Fig. 5; in addition each point $q \in Q_0$ for which $F(q) \notin Q_0$ has $F^2(q)$ to the right of \bar{x}_0 , and the same is true of $F^n(q)$ for all $n \geq 2$, since once a point is to the right of $L(\bar{x}_0)$, it must stay to the right. The curve shown is the image of this segment shown at $x = x_0$.

We write $F(\infty) = \infty$. It automatically follows that F is a homeomorphism on \mathbb{R}^2 , since it must be continuous at ∞ . We assume throughout this section that F satisfies the following assumptions:

A1. F is area-preserving.

A2. Periodicity assumption. If we write $(\bar{x}, \bar{y}) = F(x, y)$, then $F(x + 2\pi, y) = (\bar{x} + 2\pi, \bar{y})$.

A3. There is a nonempty invariant set S , i.e., $F(S) = S$, such that there is a uniform bound σ on $|y|$ for all $(x, y) \in S$. Also, $(x, y) \in S$ implies $(x + 2\pi i, y) \in S$ for all $i = 0, \pm 1, \pm 2, \dots$. For purposes of the Sec. III, we assume there is a uniform $\delta > 0$ such that if $(x, y) \notin S$, then the

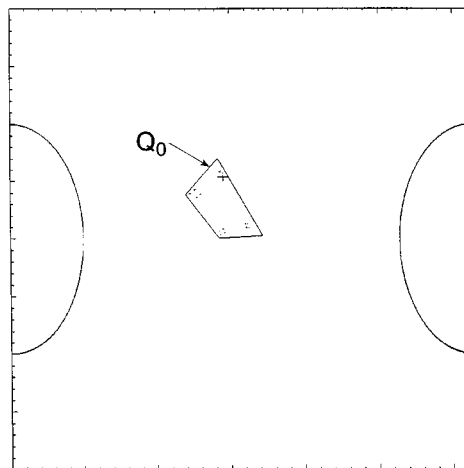


FIG. 10. The points shown inside the quadrilateral Q_0 constitute the Cantor set, whose trajectories of points remain inside Q_0 for all time $t = 0, \pm 1, \pm 2, \dots$.

x -coordinate of $F(x, y)$ is greater than $x + \delta$; that is, everywhere outside the strip S , the fluid moves uniformly to the right.

A4. Let $L(x_0)$ be the vertical line with x -coordinate x_0 . There is a value x_0 such that F maps each point on $L(x_0)$ strictly to the right of $L(x_0)$.

Remark. This indicates the flow is generally from left to right. For our example in the introduction, x_0 can be chosen to be zero or to be the line in Fig. 5 (or even \bar{x}_0 in Fig. 8).

A5. We assume there is a quadrilateral Q_0 , which has the following **lockout** property. That is, if $q \in Q_0$ and for some $k > 0$, $F^k(q) \notin Q_0$, then further iterates of q remain outside Q_0 ; i.e., $F^n(q) \notin Q_0$ if $n \geq k$. We assume Q_0 lies between $L(x_0)$ and $L(x_0 + 2\pi)$.

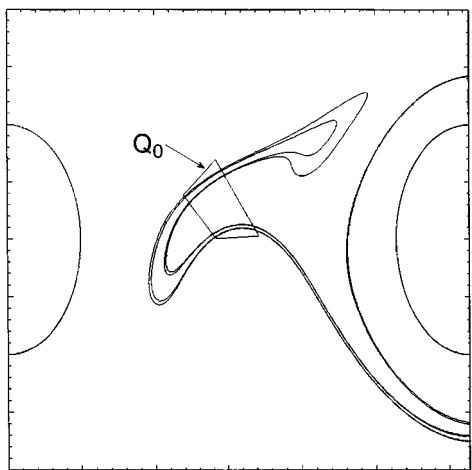


FIG. 9. This picture shows the first iterate $F(Q_0)$ of the quadrilateral, which is also $G^2(x, y)$.

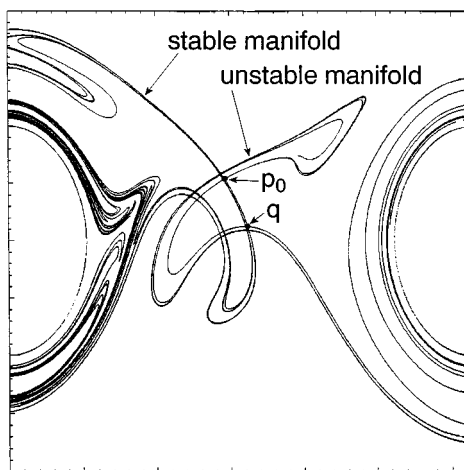


FIG. 11. The horseshoe F on Q_0 in Fig. 9 has some isolated fixed points. One of these p_0 is shown here. The stable and unstable manifolds of p_0 intersect at a point $q \neq p_0$ other than p_0 . The closure of the set of such intersection points is the Cantor set shown in Fig. 10, and it was created by plotting the intersections.

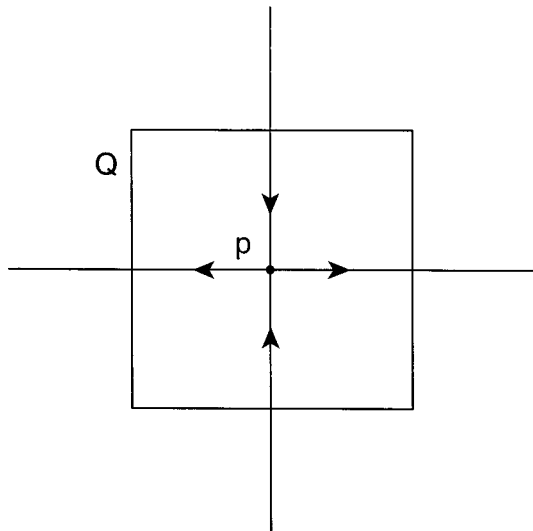


FIG. 12. This quadrilateral Q , under the linear map $(x,y) \rightarrow (2x,y/2)$, contains a saddle fixed point p in its interior. It satisfies the lockout property: once a point leaves Q , it cannot return.

Remark. See Fig. 12 for a trivial example of a quadrilateral Q that satisfies the lockout property.

A6. F is a horseshoe map on Q_0 . Write A, B, C, D for the vertices of Q_0 as in Fig. 13. We do not give a full definition here, but we assume F is hyperbolic horseshoe map in the sense of Smale.² In particular if $G: \mathbb{R}^2 \rightarrow \mathbb{R}^2$ is a horseshoe map on Q_0 , then the top DC and bottom AB have images $G(AB)$ and $G(CD)$ that lie outside Q_0 and the image $G(Q_0)$ of Q_0 stretches at least twice across Q_0 as shown in Fig. 13, without intersecting sides AD or BC . Also for almost every $q \in Q_0$ there is an $n > 0$ depending on q for which $G^n(Q_0) \not\subset Q_0$. It follows that every horseshoe map must contain at least two saddle fixed points. We will let p_0 denote any one of these.

Remark. Recall that in our example there is a map G with the property that $F = G^2$ and our numerical calculations show that G is a horseshoe map for which $G(Q_0)$ stretches twice across Q_0 (see Fig. 6) and F is also a horseshoe on Q_0 , and $F(Q_0)$ stretches four times across Q_0 (see Fig. 9).

2.1 Proposition. For almost every $q \in Q_0$, we have $F^n(q) \rightarrow \infty$ as $n \rightarrow \infty$, and in particular the x -coordinate of $F^n(q)$ tends to $+\infty$ as $n \rightarrow \infty$.

Sketch of proof. Let B be the set $F(Q_0) - Q_0$. Then B consists of points that have just left Q_0 and $F(B)$ consists of the points that left Q_0 exactly two iterates before. Since F is one-to-one, if $b \in B$, then $b \notin Q_0$, and so $F(b) \notin B$. In other words $F(B)$ is disjoint from B . By the lockout property, $F(B)$ is also disjoint from Q_0 . Applying the same argument shows $F^k(B)$ is disjoint from $B, F(B), \dots$, and $F^{k-1}(B)$. But each of these disjoint sets have the same area as B , because F is area-preserving. Let V be the rectangle in \mathbb{R}^2 defined by $x \in [x_0 - 2\pi n, x_0 + 2\pi n]$ for some $n \geq 1$ and $|y| \leq \sigma$, where x_0 is as in A4 and σ is as in A3. In particular $Q_0 \subset V$. Let $B_V \subset B$ be the set such that $b \in B_V$ implies that $F^n(b) \in V$ for all $n > 0$. We claim B_V has area 0. The sets

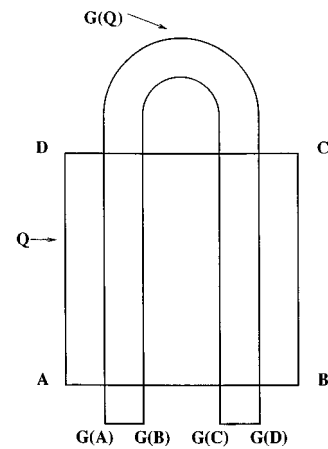


FIG. 13. This figure shows the topological horseshoe map. In particular here $G(Q)$ stretches twice across Q and the top and bottom sides CD and AB are mapped entirely outside of Q .

$B_V, F(B_V), F^2(B_V), \dots$, are disjoint because $F^k(B_V) \subset F^k(B)$. Furthermore all $F^k(B_V)$ have area equal to the area of B_V . Since all $F^k(B_V)$ lies in V ,

$$\text{area}(V) \geq \sum_{k=1}^{\infty} \text{area}(F^k(B_V)) = \infty \times \text{area}(B_V). \quad (1)$$

Hence the area of B_V is 0, since otherwise the union of all $F^k(B_V)$ would have infinite area, proving the claim. It follows that for almost every $q \in Q_0$ the trajectory of q eventually leaves V . By construction of V , it can only leave through the right end, and can never return to V because A4 applies to $x_0 + 2\pi n$. Since this holds for every n , $F^n(q)$ has x -coordinate tending to $+\infty$, and $F^n(q) \rightarrow \infty$ as $n \rightarrow \infty$.

Definition of Λ_0 . We define the set Λ_0 to be the closure in \mathbb{R}^2 of the set $\{u: F^{-n}(u) \text{ is in } Q_0 \text{ for all sufficiently large } n\}$. This set can be viewed as the limit points of the family of sets $Q_0, F(Q_0), F^2(Q_0), \dots$. We remark that Λ_0 is the closure of the unstable manifold of p_0 (different saddles in Q_0 yield the same Λ_0), where p_0 is defined in A6.

2.2 Theorem. Λ_0 is an indecomposable continuum.

Remark. This result is based on ideas of M. Barge³ who proved under additional mild assumptions that if a saddle fixed point has stable and unstable manifolds that intersect, then the closure of one of the branches of the unstable manifold is an indecomposable continuum.

By the periodicity assumption A2, the x values $x_0 + 2\pi i$ satisfies A4 for all $i = 0, \pm 1, \pm 2, \dots$. Hence we will assume x_0 lies to the left of Q_0 . We address how the set Λ_0 is related to $S^+(x_0)$ defined in the introduction. The boundary of a compact set S , written $\text{bdy}(S)$, is $S - \text{interior}(S)$; if S has no interior, then $S = \text{bdy}(S)$. In our example it appears as though Λ_0 equals $\text{bdy}(S^+(x_0))$. These sets $S^+(x_0)$ and Λ_0 differ significantly in that $S^+(x_0)$ contains the cylinders and the invariant bubbles such as those of Fig. 7. We conjecture that here $\Lambda_0 = \text{bdy}(S^+(x_0))$. Our hypotheses imply the following results.

2.3 Proposition. The continuum Λ_0 is contained in $\text{bdy}(S^+(x_0))$.

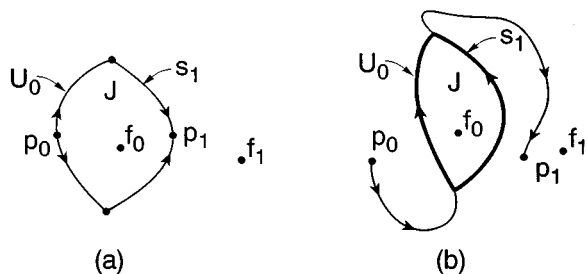


FIG. 14. Assumption A8 requires the segments U_0 and S_1 to separate one fixed point f_0 from another f_1 . Two possible configurations are shown.

Remarks. Notice that since p_0 is to the right of x_0 , its unstable manifold lies completely to the right of x_0 by A4, so $\Lambda_0 \subset S^+(x_0)$. From the definition of a horseshoe map, it follows that F^{-1} is also a hyperbolic horseshoe map on Q_0 , and consequently the closure of the stable manifold of a fixed point p_0 in Q_0 is an indecomposable continuum. Note that F^{-1} automatically satisfies the lockout property.

We define Q_i , Λ_i , and p_i to be the horizontal translates by $x = 2\pi i$ of Q_0 , Λ_0 , and p_0 , respectively. These inherit properties because of the periodicity assumption A2. In particular F is a horseshoe map on Q_i ; Q_i satisfies the lockout property; p_i is a saddle fixed point in Q_i ; and Λ_i is the closure of the unstable manifold of p_i and is an indecomposable continuum. While there are no assumptions in this section about cylinders, it is useful to define C_i as the horizontal translate of a particular cylinder C_0 by $2\pi i$. So we ask then how the indecomposable continua are related to each other. We add another assumption.

A7. The unstable manifold of p_0 crosses the stable manifold of p_1 .

2.4 Proposition. *The continuum Λ_{i+1} is contained in, but is not equal to Λ_i .*

Sketch of the proof. First we argue that Λ_i and Λ_{i+1} are unequal. By A5, the line $L(x_0 + 2\pi(i+1))$ in A4 lies strictly between p_i and p_{i+1} . Hence Λ_{i+1} does not contain p_i , but Λ_i does, so they are not equal. The proof that $\Lambda_i \supset \Lambda_{i+1}$ follows from the so-called Lambda Lemma,⁴ using assumption A7.

The figures in the introduction suggest the indecomposable continua in our example are quite complicated. In fact Λ_0 seems to separate the plane into many regions, and in particular we can prove this with the following assumption.

A8. Assume that there is a connected segment U_0 of the unstable manifold of p_0 and a connected segment S_1 of the stable manifold of p_1 . Assume U_0 and S_1 have the same end points and together they bound a region J that contains some fixed point f_0 in its interior but excludes another fixed point f_1 (as shown in Fig. 14).

2.5 Theorem. *Each connected path from f_0 to f_1 must intersect Λ_0 .*

Remark. In our example, the cylinders consist of fixed points. If we choose f_0 to be any point of one cylinder and f_1 a point of the next cylinder, Fig. 15 shows numerically

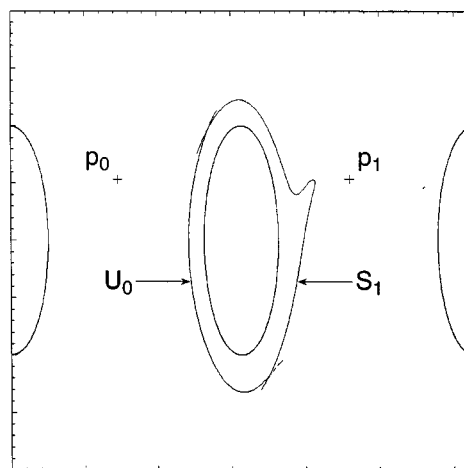


FIG. 15. This figure shows that the assumption A8 is satisfied by our example. The cylinder is encapsulated by the segments of the stable and unstable manifolds of the fixed points p_1 and p_0 , respectively. The fixed point f_0 in Theorem 2.5 can be any point of the cylinder and f_1 is any point of any other cylinder. Of course all cylinder points are automatically fixed points. This configuration is like in Fig. 14(b) in that the fixed points p_0 and p_1 are not in the segments used for encapsulation.

that our example has the property A8. Of course all the points of the cylinders are fixed points.

Sketch of the proof. Suppose there is a path γ from f_0 to f_1 that does not intersect Λ_0 . Then γ must intersect S_1 . There is another similar picture obtained by applying F to U_0, S_1, J, f_0 , and f_1 . Since f_0 and f_1 are fixed points and $f_0 \in J$ and $f_1 \notin J$, it follows that $f_0 \in F(J)$ and $f_1 \notin F(J)$ and $F(J)$ is bounded by $F(S_1)$ and $F(U_0)$. Hence we have another geometry equivalent to the first, and it follows that γ must pass through $F(S_1)$. Applying the argument again repeatedly, we find γ must pass through $F^n(S_1)$. Since these segments are shrinking and converge to p_1 , the path γ comes arbitrarily close to p_1 , so by compactness it must pass through p_1 . But p_1 is in Λ_0 by proposition 2.4. Therefore we have a contradiction to our supposition. Hence no such path γ exists.

III. PERTURBATIONS OF THE SYSTEM: THE FISH FACTOR

Assume F satisfies the hypotheses A1–A8. We consider a new assumption.

B1. Let $\epsilon > 0$. Assume that instead of applying F at each time i , we instead require that for each i , we have an area-preserving homeomorphism F_i of \mathbb{R}^2 which is close to F in the sense that $|F(q) - F_i(q)| < \epsilon$ and $|DF(q) - DF_i(q)| < \epsilon$ for each i and q . We refer to ϵ as the “noise level.”

The only assumption about F_i is B1. All conclusions must follow from our assumptions about F and from the fact that the noise level ϵ is sufficiently small.

For an unperturbed system, we define the trajectory through any q_0 to be $q_n = F^n(q_0)$ and this holds for all n positive and negative. For our perturbed system, we always discuss initial points at time zero for simplicity. Then $F(q_0)$ is replaced by $F_0(q_0)$ and $F^2(q_0)$ is replaced by

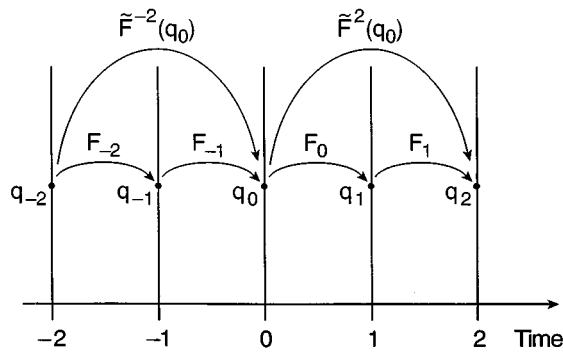


FIG. 16. The trajectory with noise through q_0 at time 0.

$F_1(F_0(q_0))$, etc., so that the *forward trajectory* of a point q_0 under the new perturbed system consists of the sequence $q_0, F_0(q_0), F_1(F_0(q_0)), \dots$. Similarly $q_{-1} = F^{-1}(q_0)$ is replaced by $F^{-1}_1(q_0)$, and q_{-2} becomes $F^{-1}_2(F^{-1}_1(q_0))$, etc., and we refer to $q_0, q_{-1}, q_{-2} \dots$, as the *backward trajectory* q_0 . Notice that automatically $F_i(\infty) = \infty$ since this is true for any homeomorphism of R^2 , that is, if $q \rightarrow \infty$ in R^2 , then it implies that $F_i(q) \rightarrow \infty$.

We write $\tilde{F}^n(q_0)$ for the analog of $F^n(q_0)$ for all n positive and negative. More precisely, for $n > 0$, we define $\tilde{F}^n(q_0)$ to be $F_{n-1}(\dots(F_0(q_0)))$ and $\tilde{F}^{-n}(q_0)$ for $F_n^{-1}(\dots(F_{-1}^{-1}(q_0)))$. In particular $\tilde{F}^n(q_0) = q_n$ for each n . See Fig. 16.

Now it no longer makes sense to talk about *invariant* Cantor sets, *invariant* points, or *invariant* continua. Perhaps we should assume $F_i(q) \equiv F(q)$ for q inside the cylinders so the cylinders themselves are still invariant, except that our results do not involve cylinders explicitly. However, we can discuss those points q in R^2 such that the backward trajectory's x -coordinates do not go to $-\infty$ or those whose forward trajectory's x -coordinates do not go to $+\infty$. The reader might be considering how we can arrive at conclusions when there are no invariants sets. Assume there is a quadrilateral Q with F linear in Q , as in Fig. 12. Then for ϵ sufficiently small, there is precisely one point q (at time 0), whose noisy trajectory \tilde{F} remains in Q for all time, positive and negative. Notice that q is not a fixed point since no fixed points exist in general for all F_i . When F is a horseshoe map on Q , this phenomenon is more complex, and F is a horseshoe map on $Q = Q_0$. Let Z_0 be those points $q \in Q_0$ for which $\tilde{F}^n(q) \in Q_0$ for all n , positive and negative.

3.1 Proposition. For $\epsilon > 0$ sufficiently small, Z_0 is a Cantor set.

Remark. The definition of ‘‘Cantor set’’ concerns only the shape and topology of the set and not the dynamics on the set.

We let $\tilde{S}^+(x_0) = \{q \in \overline{R^2} : \text{either } q = \infty \text{ or the trajectory } \tilde{F}^n(q) \text{ through } q \text{ at time zero remains to the right of } x_0 \text{ for all time, positive and negative}\}$. We similarly define $\tilde{S}^-(x_0)$, except that the trajectories remain to the left of x_0 for all time. We claim that for every x_0 , $\tilde{S}^+(x_0)$ contains an

indecomposable continuum, and so does $\tilde{S}^-(x_0)$.

Definition of $\tilde{\Lambda}_0$. We define $\tilde{\Lambda}_0$ to be the closure in $\overline{R^2}$ of the set $\{u : \tilde{F}^{-n}(u) \text{ is in } Q_0 \text{ for all sufficiently large } n\}$.

We analogously define $\tilde{\Lambda}_i$ using Q_i instead of Q_0 . Since F_i is not assumed to satisfy the periodicity assumption A2, $\tilde{\Lambda}_i$ is not in general a translate of $\tilde{\Lambda}_0$, though we expect it could nearly be a translate by $2\pi i$. In particular each $\tilde{\Lambda}_i$ is compact.

The challenge here is to identify hypotheses that are verifiable and are preserved under small perturbations of F . Assumption A5 is not a hypothesis that is preserved under small perturbations. We add the following strengthened version of A5.

A5'. There is an $\bar{x}_0 \in (x_0, x_0 + 2\pi)$ such that $L(\bar{x}_0)$ satisfies A4 and $L(\bar{x}_0)$ lies to the right of Q_0 and there is an integer N with the property that if $q \in Q_0$ and $F(q) \notin Q_0$, then $F^N(q)$ is to the right of $L(\bar{x}_0)$.

Remark. The integer N must be independent of the choice of q . Once a trajectory point moves to the right of \bar{x}_0 , it cannot return to the left, so it cannot return to Q_0 . In our example we can find such a line (Fig. 8) with $N=2$. Assumption A5' implies that for noise level ϵ sufficiently small, the lockout property holds for noisy trajectories, that is trajectories of \tilde{F} .

The horseshoe map property A6 is automatically preserved under small perturbations, so each F_i is a horseshoe map on each Q_i for small ϵ .

3.2 Theorem. For $\epsilon > 0$ sufficiently small, each $\tilde{\Lambda}_i$ is an indecomposable continuum.

3.3 Proposition. For $\epsilon > 0$ sufficiently small, the continuum $\tilde{\Lambda}_0$ is contained in $\text{bdy}(\tilde{S}^+(x_0 + 2\pi i))$.

3.4 Theorem. For $\epsilon > 0$ sufficiently small, for each i the continuum $\tilde{\Lambda}_{i+1}$ is contained in, but is not equal to $\tilde{\Lambda}_i$.

Remark. Recall from the assumption A8 that the points f_0 and f_1 are fixed points for F , but presumably not for F_i .

3.5 Theorem. For $\epsilon > 0$ sufficiently small, each connected path from f_0 to f_1 must intersect $\tilde{\Lambda}_0$.

The proofs of these results will be published elsewhere.

IV. LAGRANGIAN DYNAMICS FOR THE FLUID FLOW

As it has been pointed out in the Introduction, instead of directly solving the corresponding Navier-Stokes equations of the fluid flow, we adopt a rather different approach. When the fluid is incompressible, as in our case, we can formulate the problem in terms of an auxiliary function, the *stream function*. In such formulation the continuity equation is immediately satisfied and can easily be applied to two-dimensional flows, axisymmetric flows and some very special cases of three-dimensional flows.

When dealing with a complex fluid flow, it is rather convenient to find ways of visualizing it. There are traditionally three ways of carrying out this task, through streaklines, streamlines, or pathlines. A streakline is the locus of fluid particles originating from the same initial point. A streamline

is a continuous and smooth curve whose tangent coincides with the velocity field at each point. The streamlines of the flow, at a given time t , are simply the level curves of constant value of the stream function. The pathlines in turn are the trajectories which follow a simple fluid particle. If the stream function is time-independent, the system is integrable and the streaklines, the streamlines, and the pathlines coincide. However, they do not coincide when the stream function is time dependent.

The equations describing the motion of fluid particles in an incompressible two-dimensional fluid flow take the form of Hamilton's equations,

$$\dot{x} = v_x \equiv \frac{\partial \psi(x,y,t)}{\partial y}, \quad \dot{y} = v_y \equiv - \frac{\partial \psi(x,y,t)}{\partial x}, \quad (2)$$

where v_x and v_y are the two components of the velocity field, and $\psi(x,y,t)$ is the time-dependent stream function that plays the role of a Hamiltonian function. The property of area-preserving in phase space is a consequence of the incompressibility of the fluid.

If the flow is steady, $\psi = \psi(x,y)$ is constant along the pathline, the system has one degree of freedom, and it is integrable. If the flow $\psi = \psi(x,y,t)$ is time-periodic with period T , the system is said to have *one and half* degrees of freedom, since time is regarded as an additional 1/2 degree of freedom, in such a way that the whole phase space is three-dimensional and does not need to be integrable. So chaos is possible.

We consider an approximate model for the stream function $\psi = \psi(x,y,t)$, which is time-periodic with period $T=1$. Our model choice provides us with reasonably faithful dynamics and is much easier to deal with and much faster computationally than solving numerically the Navier-Stokes equation for the problem. The model introduced in⁵ and used in^{6,7} for the fluid flow past one single cylinder is extended here for the fluid flow past an infinite periodic array of cylinders.

The parameters involved in the modeling are the following:

- (i) The frequency $\phi = 2\pi$ of the velocity field.
- (ii) The size ρ , where $\rho^{-1/2}$ is the characteristic linear size of the vortices.
- (iii) The width σ , where $\sigma^{-1/2}$ play the role of the boundary layer at the cylinder.
- (iv) The ratio α of vortex size in x to size in y .
- (v) The height y_0 of the center of the vortices.
- (vi) The distance d , where $d\pi$ is the distance between cylinder centers.
- (vii) The strength $\omega = 24$ of the vortices.
- (viii) The velocity $\beta = 14$ of the background flow.

The following parameters choice has been used throughout all the numerical computations: $\rho = 0.35$, $\sigma = 1.0$, $\alpha = 2.0$, $L = 2.0$, $y_0 = 0.3$, $d = 2.0$, $\omega = 24$, and $\beta = 14.0$. The centers of the cylinders are at $x = 0, \pm 2\pi, \pm 4\pi, \dots$. This set of parameters provides a rather good agreement with a known solution of the Navier-Stokes equations in the case of

fluid flow behind one cylinder.^{6,7} In fact for the Navier-Stokes equations, the boundary layer near the cylinder is quite thin, but in our system we have made the boundary thicker as in.^{6,7} The stream function $\psi(x,y,t)$ of the model is defined by

$$\psi(x,y,t) = f(x,y)g(x,y,t), \quad (3)$$

where the function $f(x,y)$ gives information about the geometrical constraints, that is, the "cylinders" for the flow; and the function $g(x,y,t)$ gives the contributions of the vortices and of the background flow. We also require for $\psi(x,y,t)$ to be a periodic function in x with a period 2π . The function $f(x,y)$ is given by

$$f(x,y) = 1 - \exp\{-\sigma[(\sin^2(x/2) + (y/2)^2)^{1/2} - 1/2]^2\}. \quad (4)$$

This form ensures that the tangential velocity tends linearly to zero as expected in a boundary layer. The radial components of the velocity vanishes quadratically, which shows that the cylinder surface can be viewed as the union of an infinite number of fixed points.

Our spatial array of "cylinders" is obtained by the locus of points (x,y) which makes $f(x,y) = 0$. In other words, for these points the stream function is identically zero on the surface of the "cylinders," yielding then the appropriate no slip boundary condition. From the above condition it is inferred that

$$\sin^2(x/2) + (y/2)^2 = (1/2)^2, \quad (5)$$

where $\phi(x,y) = \sin^2(x/2) + (y/2)^2 - (1/2)^2$ is a periodic function in x of period 2π . The function $f(x,y)$ is 0 on the surface and has gradient 0 there. We redefine $f(x,y)$ so that inside the cylinders it is identically 0. The stream function $\psi(x,y,t) = f(x,y)g(x,y,t)$ will inherit these properties from $f(x,y)$. Our array of "cylinders" is periodic in x with period 2π and each "cylinder" has a vertical radius of 1 and a horizontal radius of 1.05, which is very close to a "real" cylinder. Since the function $f(x,y)$ depends only on the parameter σ , there is only one way to modify this function: by modifying the width of the boundary layer (σ).

We begin by defining $g(x,y,t)$ only for x in $[0, 2\pi]$. It is constructed so that $g(x,y,t)$ has the same values at $x=0$ and at $x=2\pi$. The equation for $g(x,y,t)$ involves two more functions $vor(x,y,t)$ and $bflow(x,y)$, which are the functions governing the vortices and the background flow, respectively, as discussed next. It is given by

$$g(x,y,t) = \sin(x/2)vor(x,y,t) + bflow(x,y). \quad (6)$$

For x in $[0, 2\pi]$ the function $vor(x,y,t)$ is defined as

$$vor(x,y,t) = \omega\{-h_1(t)g_1(x,y,t) + h_2(t)g_2(x,y,t)\}, \quad (7)$$

where

$$g_i(x,y,t) = \exp\{-\rho\{[x-x_i(t)]^2 + \alpha^2[y-y_i(t)]^2\}\}. \quad (8)$$

The function $vor(x,y,t)$ is responsible for the birth and death of vortices and it depends on the strength of the vortices ω , the functions $h_1(t)$ and $h_2(t)$, which in turn depend on the frequency ϕ , and the functions $g_1(x,y,t)$ and $g_2(x,y,t)$. The functions $g_1(x,y,t)$ and $g_2(x,y,t)$ depend on

ρ , which are related to the characteristic linear size of the vortices; and α is the ratio of vortex size in x to size in y . The functions $g_1(x,y,t)$ and $g_2(x,y,t)$ depend also on the vortex centers, which in turn depend on L , the distance that vortices travel before dying out, and y_0 , the height of the center of the vortices. Hence, the function $vor(x,y,t)$ may be changed by modifying either the: strength ω of the vortices, frequency ϕ of the velocity field, vertical size ρ of the vortices, ratio α of vortex size in x to size in y , height y_0 of the center of vortices, or distance L that vortices travel before dying out.

The flow is time-periodic with period 1 and this allows us to define

$$h_1(t) = \left| \sin\left(\frac{\phi t}{2}\right) \right|, \quad h_2(t) = h_1(t - 1/2). \quad (9)$$

This implies that $vor(x,y,t)$ creates two vortices between the cylinders at $x=0$ and $x=2\pi$, with the functions $g_1(x,y,t)$ governing one vortex and $g_2(x,y,t)$ governing the other.

The vortex centers move parallel to the x -axis with constant velocity. The x -coordinates change with time and are given by

$$x_1(t) = 1 + L[t \bmod 1], \quad x_2(t) = x_1(t - 1/2). \quad (10)$$

Hence the x vortices at x_1 and x_2 are each created periodically in time with period 1. The y coordinates, on the other hand, are constant, with y_1 and y_2 given by

$$y_1(t) = -y_2(t) \equiv y_0. \quad (11)$$

There are thus two vortices, and their behavior entails traveling a distance L during a period and then dying out.

The function $bflow(x,y)$ is defined as

$$bflow(x,y) = \beta y s(x,y), \quad (12)$$

where $s(x,y)$ depends on the vortex ratio α and is given by

$$s(x,y) = 1 - \exp\left\{-\frac{1}{\alpha^2}[x - 1.05]^2 - y^2\right\}. \quad (13)$$

It expresses the contribution of the background flow with uniform velocity β , while the function $s(x,y)$ is introduced to simulate the *shielding* of the background flow right behind the cylinder. One of the features of this function is that it is identically zero at the rightmost point of each cylinder. The function $bflow(x,y)$ may be changed by modifying the: ratio α of vortex size in x to size in y , or velocity β of the background flow.

So far $g(x,y,t)$ has been defined for $0 \leq x \leq 2\pi$ and it has the important property that it has the same values at $(0,y,t)$ and $(2\pi,y,t)$. Hence we can make it a continuous periodic function of x with period 2π . We take $[0,2\pi]$ to be a fundamental period for x and define $g(x,y,t)$ as follows. Choose n so that $x - 2\pi n$ is between 0 and 2π . Then define

$$g(x,y,t) = g(x - 2\pi n, y, t). \quad (14)$$

Hence $g(x,y,t)$ is periodic in x with period 2π .

V. CONCLUDING REMARKS

We have explored a numerical example of a fluid flowing past an array of cylinders. While one can rigorously prove that the flow preserves area, almost all of our observations lack rigor. Furthermore we have not studied the Navier-Stokes equations, but rather the computationally much simpler Lagrangian dynamics of a stream function we have imposed. This is similar to the physician who studies cancer in mice rather than people. We would prefer to study the Navier-Stokes equations. Our solution to this quandary is to present rigorous results that are logically independent of our numerical example. The hypotheses are suggested by the example but will also be true in many other fluid flows. Our goal is to study fluid flow which is a periodic flow plus a time varying perturbation. Under such circumstances, no bounded invariant sets are preserved (except the cylinders). We show that it is nonetheless possible to discuss fractal sets that remain. These are often indecomposable sets which correspond to physically observable remnants of dye introduced earlier into the fluid.

ACKNOWLEDGMENTS

Most of the figures have been created using the DYNAMICS software.⁸ Miguel A. F. Sanjuan acknowledges a grant of the Spanish Ministry of Education (DGICYT PR95-091). This work was also supported by the National Science Foundation (Mathematical Sciences Division) and the U.S. Department of Energy (Office of Scientific Computing).

APPENDIX A: BASIC CONCEPTS OF INDECOMPOSABLE CONTINUA

Most scientists working in dynamics are aware that the limit sets associated with dynamical systems can be quite complicated. This section discusses some of the topological structures of dynamics and shows how far from the usual Euclidean intuition these sets can be. The structure that interests us most here is an object known to topologists as an *indecomposable continuum*. While understanding these requires gaining a different intuition than most mathematicians and scientists possess, the good news is that these objects have been studied since the early part of this century, and there exists a considerable body of literature on them. A brief history of indecomposable continua can be found in Ref. 1. Also, even though they must be dealt with on their own terms, they do have structure. That structure is quite rich, with strong rules governing their behavior.

We write $\overline{R^2} = R^2 + \{\infty\}$ to denote the one point compactification of the plane, in such a way that it is topologically equivalent to the two dimensional sphere S^2 . More generally we can write $\overline{R^n} = R^n + \{\infty\}$ to be the one point compactification of R^n .

A closed set A in $\overline{R^2}$, is said to be *connected* if it cannot be written as the union of two disjoint, closed nonempty sets. A *continuum* K in $\overline{R^n}$ is defined as a compact, connected subset of $\overline{R^n}$. In particular $\overline{R^n}$ is a continuum. If X and Y are

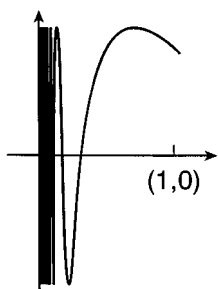


FIG. 17. The topologist's $\sin(1/x)$ curve.

spaces (or subsets of a space such as R^n), $h: X \rightarrow Y$ is one-to-one, continuous, and onto, and h^{-1} is also continuous, then h is a *homeomorphism*. In these circumstances the sets X and Y are said to be *homeomorphic*, or *topologically equivalent*. An *arc* is a set that is homeomorphic to the unit interval. A set X is *arcwise connected* if for each pair p, q of points in X , there is an arc contained in X that contains both p and q . If Y and X are continua, and $Y \subseteq X$, then we say Y is a *subcontinuum* of X . If in addition $Y \neq X$, then we say that Y is a *proper subcontinuum* of X .

(1) *A remark and an example.* Every continuum in R^1 is an arc or a point, and therefore every continuum in R^1 is arcwise connected. However, this is *not* true for subsets of higher-dimensional spaces. Probably the simplest example of a continuum that is *not* arcwise connected is the *topologist's sine curve* X in the plane, see Fig. 17. Define X_0 to be $\{(x, y) \in R^2: 0 < x \leq 1 \text{ and } y = \sin(1/x)\}$ and X_1 to be the vertical line segment with $x=0$ and $-1 \leq y \leq 1$. Then X_1 is contained in the closure of X_0 in R^2 , and $X = X_0 \cup X_1$ is the continuum pictured in Fig. 17. Note that $(0,1)$ and $(1, \sin(1))$ are in X , but there is no arc from $(0,1)$ to $(1, \sin(1))$ that is contained in X .

(2) *Remark.* Any open, connected subset of R^n is arcwise connected.

A set X is said to be *locally connected* if each point has "arbitrarily small" neighborhoods that are connected. More precisely, if for each neighborhood U of any point p in X there is a connected neighborhood V of p such that $V \subset U$, then X is locally connected. The interval $[-1, 1]$ is connected. If we remove the point $\{0\}$, what remains is not connected but is locally connected.

(3) *Example.* Begin with the middle-thirds Cantor set C sitting on the unit interval $[0, 1]$ on the x axis in the plane. The *middle-thirds Cantor set* C is the set which remains after iteratively removing the middle-third of the unit interval and of every remaining subinterval, see Fig. 18. The *Cantor fan* consists of the middle-thirds Cantor set, the point at $(1/2, 1)$ plus the line segments that run from each point of the Cantor set to $(1/2, 1)$.

The Cantor fan, pictured in Fig. 19, is a continuum in R^2 which is arcwise connected, but is not locally connected. Note that it is locally connected at the point $(1/2, 1)$ [that is, there are arbitrarily small connected neighborhoods of $(1/2, 1)$ contained in the Cantor fan] although it is not locally

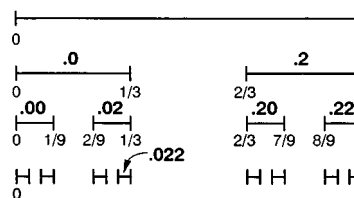


FIG. 18. Construction of the middle-third Cantor set. In step 1, the middle third of the unit interval is removed. In further steps, the middle third of every remaining subinterval is removed. Here three steps are shown. The points that are never removed make up the Cantor middle-third set. The set marked 0.02 consists of all numbers in the unit interval whose ternary expansion begins with 0.02.

connected at any other point. The topologist's $\sin(1/x)$ curve is locally connected at each point of X_0 , but it is not locally connected at any point of X_1 . There is no arc in X that connects a point of X_1 to a point of X_0 , even though points of X_0 can be found in each neighborhood of each point of X_1 .

(4) *Remark.* While it is not immediately obvious, the following is true. Every connected, locally connected, subset of R^n is arcwise connected. Example 3 demonstrates that the converse to this statement is not true.

Suppose X is a continuum and A is a closed subset of X . A component K of A is a connected subset of A which is not a proper subset of any other connected subset of A . Each point of A is contained in a component of A , though in some cases the component might be just a single point.

(5) *Example.* Suppose that D is a closed disk in R^2 (i.e., a circle and its interior). Suppose that X denotes the topologist's $\sin(1/x)$ curve and M denotes the Cantor fan. What do the components of $D \cap X$ and $D \cap M$ look like, assuming the intersection is nonempty and it is not all of X or M ? It depends, of course, on which D is considered, but assuming $(1/2, 1) \notin D$ and X_1 is not a subset of D , each component of $D \cap X$ or $D \cap M$ is an arc or a point. Further, if we are considering $D \cap X$, and the interior of D contains a point of X_1 , then $D \cap X$ has countably infinitely many components, all but one of which is an arc. (See Fig. 20).

If we consider $D \cap M$ and $(1/2, 1) \notin D$, then all, except possibly one, of the components of $D \cap M$ are arcs and there are uncountably many components in $D \cap M$. On the other hand, if $(1/2, 1)$ belongs to the interior of D , then $D \cap M$ is itself a continuum homeomorphic to M . In this case $D \cap M$ has only one component.

Neither X nor M is an *indecomposable continuum*, but we are heading in that direction. Indecomposable continua are not arcwise connected and they are not locally connected

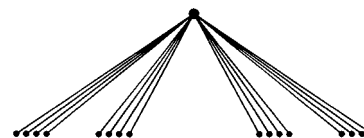


FIG. 19. Cantor fan.

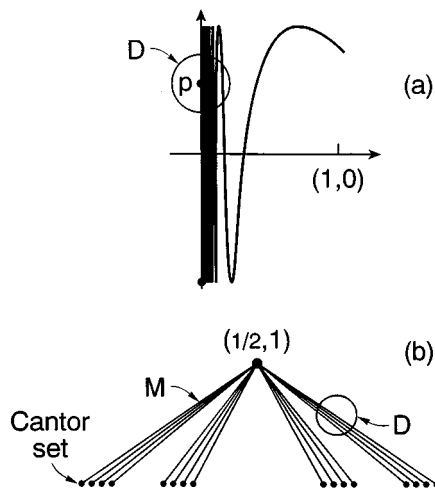


FIG. 20. (a) $D \cap X$ with $X \cap$ interior of D , nonempty. (b) The Cantor fan M . Here D intersects M with $(1/2, 1) \notin D$, and $M \cap$ interior of D nonempty.

at any point. The invariant set for the canonical Smale horseshoe map is a simple example of an indecomposable continuum, and we recall the construction of that example below:

(6) *Example. The invariant set of the Smale horseshoe map.*² The construction begins as follows: Consider the stadium-shaped region called D in Fig. 21(a). The set D consists of a rectangle R with interior, and two semicircles A and B (interiors included), that are sewn onto the shorter sides of R . Now $D \subseteq \mathbb{R}^2$ and the homeomorphism F on \mathbb{R}^2 maps D into itself as pictured in Fig. 21(b). Think of F having the following effect on D : the map F shrinks D vertically, stretches D horizontally, contracts the semicircle regions A and B , and then folds the shrunk, stretched, contracted D once and places the acted-upon D back into itself so that $F(A)$ and $F(B)$ are in the interior of A , $F(R)$ is in the interior of D , and $F(R)$ intersects B in a nontrivial way.

Since $F(D) \subset D$, $F^2(D) = F(F(D)) \subset F(D)$. Figure 22 shows the second iteration of D , that is $F^2(D)$. This process continues: $D \supseteq F(D) \supseteq F^2(D) \supseteq \dots$. Since each $F^n(D)$ is a

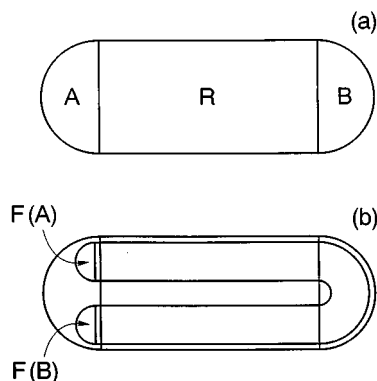


FIG. 21. (a) The stadium region D . (b) The horseshoe map on D .



FIG. 22. $F^2(D)$ in $F(D)$ and D .

continuum, the sequence $D, F(D), F^2(D), \dots$ is a sequence of nested continua. An elementary theorem from topology tells us that the intersection of nested continua is itself a continuum. Then it follows that $K = \bigcap_{n=1}^{\infty} F^n(D)$ is a continuum.

Now another theorem from topology states that any nested intersection of compact sets is nonempty and compact. Since $K \cap A$ can be written $\bigcap_{n=1}^{\infty} [F^n(D) \cap A]$ and $K \cap B$ can be written $\bigcap_{n=1}^{\infty} [F^n(D) \cap B]$, it follows that $K \cap A$ and $K \cap B$ are both nonempty. Thus, K contains more than one point. A continuum that contains more than one point is said to be *nondegenerate*. Note that if $q \in \mathbb{R}^2$ and there is some positive integer n such that $F^n(q) \in D$, then the sequence $q, F(q), F^2(q), \dots$ must be getting closer and closer to K . In other words, K is the global attractor for D in the sense that all initial points are attracted to K . The continuum K , so defined, represents the invariant set of the Smale horseshoe map and is also an indecomposable continuum.

Precisely, a continuum X is *decomposable* if it can be written as the union of two proper subcontinua H and K . The sets H and K must overlap. A continuum that is not decomposable is *indecomposable*. The most commonly encountered continua are decomposable (or so one might believe). For example, the interval $[0, 1]$ is the union of the two proper subcontinua $[0, 1/2]$ and $[1/2, 1]$. Giving a rigorous proof that K is indecomposable is tedious. We instead attempt to give the reader an intuitive idea of what this all means. First, it may help to think of K in another way. A set which is topologically equivalent to K is called the Knaster bucket handle, usually denoted K_2 , and it may be described as follows. (See Fig. 23 for a sketch.) Suppose C denotes the middle-thirds Cantor set sitting on the unit interval $[0, 1] \times \{0\}$ in the plane. Connect the points of C with semicircles as follows: (1) For each pair p, q of points of C such that p and q are equidistant from $(1/2, 0)$, connect p and q with a semicircle sitting above

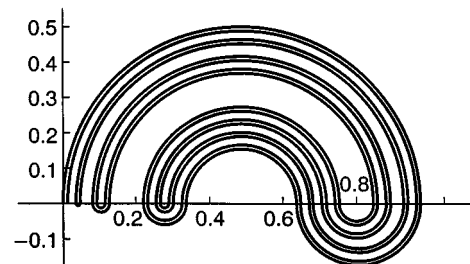


FIG. 23. The Knaster bucket handle.

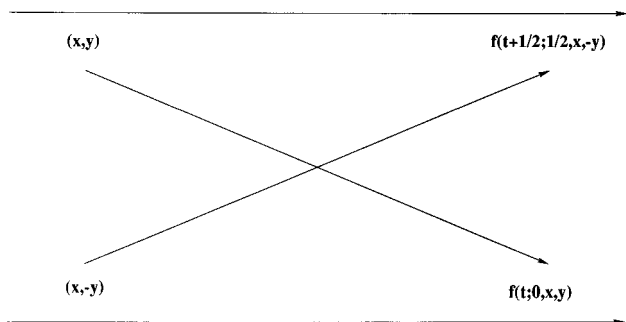


FIG. 24. This diagram shows the map of period 1/2 which maps a point of coordinates (x,y) and a symmetric one $(x,-y)$ under iteration of f .

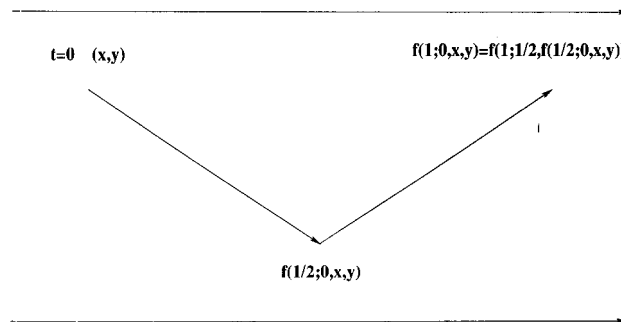


FIG. 25. This diagram shows how the point of coordinates (x,y) moves under the action of the map f .

the x axis. (2) For each pair p,q of points of C equidistant from $(5/6,0)$ [the midpoint of $(2/3,0)$ and $(1,0)$], connect p and q with a semicircle that extends below the x axis. (3) For each pair p,q of points of C equidistant from the midpoint $(5/18,0)$ of $(2/9,0)$ and $(1/3,0)$, connect p and q with a semicircle that extends below the x axis. Continue this process until the n th step which consists of connecting each pair p,q of points of C equidistant from the midpoint $(5/2(3^n),0)$ of $(2/3^n,0)$ and $(1/3^{n-1},0)$. The points p and q are to be connected with a semicircle that extends below the x axis. We emphasize that although we give no proof here that K and K_2 are topologically equivalent, comparing both constructions after rotating K_2 by 90° clockwise should at least convince the reader of the plausibility of this equivalence.

Now suppose S is a small closed disk in the plane. If the interior of S intersects K_2 , then $S \cap K_2$ consists of an uncountable collection of arcs (and possibly a couple of points on the boundary). If S intersects the interior of the Cantor fan M , and $(1/2,1)$ is not in S , then $S \cap M$ also is an uncountable collection of arcs, with possibly a couple of points on the boundary. Locally then, except around the vertex point $(1/2,1)$, M and K_2 are the same topologically. However, there is one way in which M and K_2 are very different, and that is the fact that M has the vertex point $(1/2,1)$ at which the whole continuum is connected, while K_2 possesses no such point. A stronger statement can be made: Suppose T is a closed set in R^2 that contains a closed disk S , and that K_2 intersects the interior of S , but K_2 is not contained in T . Then $K_2 \cap T$ has uncountably many components. In this case, each component is either a point or an arc. This uncountable component property is the one that makes K_2 indecomposable and M decomposable. Again, no matter where the interior of S intersects K_2 , as long as K_2 is not a subset of T , it follows that $K_2 \cap T$ has uncountably many "pieces." On the other hand, there is one point of M where this sort of property does not hold, namely at the vertex point $(1/2,1)$.

The first indecomposable continuum was discovered in 1910 by the Dutch mathematician Luitzen E. J. Brouwer as a counterexample to a conjecture of the German mathematician Arthur Schoenflies that the boundary between two connected open plane sets had to be decomposable. At first these objects were studied as examples of extreme pathology, but

by the 1920s, members of the fine Polish school of mathematics had begun to study them as interesting objects in themselves. From the discussion thus far it follows that all proper subcontinua contained in an indecomposable continuum must be nowhere dense in that continuum, i.e., no such subcontinuum can have interior relative to the indecomposable continuum. One might be tempted to believe that each such proper subcontinuum would have to be itself a simple continuum such as an arc. This is far from the case. It is far from true in the examples in this paper, and it is far from true in general. *In our cylinder flow example, each indecomposable continuum contains an infinite number of proper subcontinua which are themselves indecomposable.* This indecomposable-continua-containing-indecomposable-continua phenomenon is common in topology. In fact, R. H. Bing⁹ proved in 1951 that most continua in R^2 , or in any Euclidean space, are indecomposable continua which have the property that all their proper subcontinua are indecomposable. Such a continuum is called a *hereditarily indecomposable* continuum. By *most* continua in R^2 , we mean that if one considers the space of all continua in R^2 , when that space of continua is endowed with the topology inherited from the Hausdorff metric, then the subset of that space consisting of the hereditarily indecomposable continua forms a residual subset of the space of continua. Note that since arcs are decomposable, hereditarily indecomposable continua cannot contain arcs.

All indecomposable continua share a certain amount of structure. Suppose that X is an indecomposable continuum and $x \in X$. Then the *composant* of x in X , denoted $Com(x)$, is the union of the set of all proper subcontinua of X which contain the point x . It is not difficult to see that if x and y are two points of X , then either $Com(x) = Com(y)$ or $Com(x) \cap Com(y) = \emptyset$. Thus, the collection of $\mathcal{C}(X) = \{Com(x) : x \in X\}$ forms a partition of the continuum X . It is always the case that $\mathcal{C}(X)$ is an uncountable collection of mutually disjoint members, each of which is dense in the indecomposable continuum. Now each proper, nondegenerate subcontinuum of K_2 is an arc, while each proper subcontinuum of a hereditarily indecomposable continuum is indecomposable. Our cylinder flow continua, on the other hand, are somewhere between these two extremes: they contain both simple continua, arcs at the very

least and they also contain proper, indecomposable subcontinua. All proper subcontinua of an indecomposable continuum must be nowhere dense in that continuum and each must be contained in one component of the continuum.

APPENDIX B: SYMMETRY OF THE HORSESHOE MAP

The fluid flow is time periodic with period 1. For any initial point (x,y) and initial time t_0 , after time t_1 the flow f maps the point (x,y) to $f(t_1;t_0,x,y)$, which represents the new (x,y) point. In particular if $t_0=0$ and $t_1=1$, we then have a smooth map $F(x,y)=f(1;0,x,y)$, which is the time-1 map.

Since we have a pair of vortices which alternate periodically, there is a certain kind of symmetry. The map F is actually the square of another map G , i.e., we can write $F(x,y)=G^2(x,y)$. Our numerical evidence strongly suggests that the map G is a horseshoe map. After each period $1/2$ a vortex is created and after another period $1/2$ a vortex is destroyed. In our model vortices move downstream, in the flow, not the time-1 map, from left to right, and they die before colliding with the next cylinder, since the parameter L of the model stream function is smaller than the distance between the cylinders. The symmetry occurs because the vortices alternate above and below the horizontal axis. More precisely, a point with coordinates (x,y) at time t_0 is mapped into $f(t;0,x,y)$, while at time $1/2$ another point starting at $(x,-y)$ is mapped into $f(t+1/2;1/2,x,-y)$. Thus, the time $1/2$ is just half the period of the fluid motion (see Fig. 24).

Our time-1 map can be considered as a composition in the following manner. Suppose we follow a trajectory from

time 0 to time 1, i.e., we start with (x,y) and then consider $f(1/2;0,x,y)$, and then from that point follow it by another time period 1, so that now the time is 1 (see Fig. 25).

Then $F(x,y)=f(1;1/2,f(1/2;0,x,y))$. So an initial point (x,y) at time 0 maps into $f(1/2;0,x,y)$ which is mapped likewise into $f(1;1/2,f(1/2;0,x,y))$. We may write $(g,h)(x,y)$ for the coordinates of $f(1/2;0,x,y)$ and then $f(1;1/2,x,y)=(g,-h)(x,-y)$. Thus, summarizing,

$$f(1/2;0,x,y)=(g,h)(x,y), \quad (\text{B1})$$

$$f(1;1/2,x,y)=(g,-h)(x,-y), \quad (\text{B2})$$

and consequently

$$f(1;1/2,f(1/2;0,x,y))=f(1;1/2,g(x,y),-h(x,y)) \quad (\text{B3})$$

$$=(g,-h)(g(x,y),-h(x,y)). \quad (\text{B4})$$

Define the map $G(x,y)$ to be $(g,-h)(x,y)$. Then $G^2(x,y)=F(x,y)$.

¹J. Kennedy, "A brief history of indecomposable continua," in *Continua*, edited by H. Cook, W. T. Ingram, K. T. Kuperberg, A. Lelek, and P. Minc (Marcel Dekker, New York, 1995), pp. 103–126.

²S. Smale, *Bull. Am. Math. Soc.* **73**, 747 (1967).

³M. Barge, *Proc. Am. Math. Soc.* **101**, 541 (1987).

⁴K. T. Alligood, T. Sauer, and J. A. Yorke, *Chaos: An Introduction to Dynamical Systems* (Springer-Verlag, New York, 1996).

⁵E. Ziemniak, C. Jung, and T. Tél, *Physica D* **76**, 123 (1994).

⁶A. Péntek, Z. Toroczka, T. Tél, C. Grebogi, and J. A. Yorke, *Phys. Rev. E* **51**, 4076 (1995).

⁷C. Jung, T. Tél, and E. Ziemniak, *Chaos* **3**, 555 (1993).

⁸H. E. Nusse and J. A. Yorke, *Dynamics: Numerical Explorations* (Springer-Verlag, New York, 1994).

⁹R. H. Bing, *Duke Math. J.* **1**, 43 (1951).